# Letters

## Current Detection and Control of Synchronous Rectifier in High-Frequency *LLC* Resonant Converter

Kangping Wang, *Senior Member, IEEE*, Gaohao Wei, Jiwen Wei, Jiarui Wu, *Student Member, IEEE*, Laili Wang, *Senior Member, IEEE*, and Xu Yang, *Senior Member, IEEE*

***Abstract*—The synchronous rectification technology is widely used to improve the efficiency of power converters in applications with low output voltage and large current. However, it is challenging to accurately control the synchronous rectifier (SR) for high-frequency and high-current *LLC* converters. This letter presents a method to detect the SR current for cycle-by-cycle SR control. The resonant current and the magnetizing current are detected through magnetic coupling, and then the SR current is obtained by subtracting the two. This method requires only a few passive components and has advantages, such as high bandwidth, strong anti-interference ability, and easy implementation. This letter illustrates the working principle and implementation of the proposed method in detail and then verifies the proposed method through experiments. The proposed method can be applied to SR control in an *LLC* circuit, suitable for high frequency and large current situations.**

***Index Terms*—Current measurement, high frequency, LLC, resonant converter, synchronous rectification.**

### I. Introduction

LLC resonant converter has been widely applied to dc–dc power conversion due to its high efficiency, soft switching, easy magnetic integration, and other advantages [1]–[3]. The use of synchronous rectification technology can further reduce the loss of the synchronous rectifier (SR) and, thus, improve the overall efficiency, which is particularly important in applications with low output voltage and large current. The ON-time of the SR needs to be precisely controlled [4]. If the turn-ON time is too late or the turn-OFF time is too early, the diode will conduct for a long time, and the loss will be large. If the turn-ON time is too early or the turn-OFF time is too late, the circulating current will be generated, resulting in an increased loss. What is more serious is that there may be a short-circuit problem if the SR control signal is not given correctly, causing the circuit to burn out.

However, it is very challenging to control the SR for high-frequency and high-current *LLC* converters accurately. The popular SR control methods include SR current-based methods and "body diode" conduction-based methods. The SR current-based method detects the SR current first and then turns ON the SR, when the SR current is greater than a certain threshold. This method can achieve cycle-by-cycle control. However, it is very challenging to detect the SR current under high frequency and large current conditions. Commonly used current detection methods, such as current transformer, Rogowski coil, and Hall sensor, need to be connected in series in the circuit or wound on wires [5], which will cause the leakage inductance and resistance of the secondary side of the transformer to increase. As a result, the voltage spike and power loss of SR will increase, which is not desired to achieve high efficiency and reliability. Much research has focused on reducing the leakage inductance and resistance of the secondary [1]. Therefore, the method of directly detecting the SR current is rarely used. One commonly used method is to detect the ON-state voltage drop of the SR, which is the product of SRs ON-resistance and current [4]. This method is widely used because of its simplicity and no additional loss. However, this method is not easy to apply in high-frequency or high-current applications. Due to the unavoidable package parasitic inductance of the SR, the measured voltage drop is the sum of the voltage drop of the ON-resistance and the parasitic inductance. The impedance of the parasitic inductance increases with frequency, which will affect the accuracy of current measurement in high frequencies. Wang and Liu [6] and He *et al.* [7] proposed to reduce the influence of the parasitic inductance by adding additional circuit components to compensate. However, the parasitic inductance depends on the device packaging and layout. For a specific design, the compensation circuit needs to be tuned, which increases the complexity and design difficulty. Moreover, in high-current applications, SR devices with low ON-resistance are preferred to reduce the conduction loss. However, the ON-state voltage drop will be very small, so it

Manuscript received July 12, 2021; revised August 15, 2021 and September 15, 2021; accepted October 8, 2021. Date of publication October 14, 2021; date of current version December 31, 2021. This work was supported in part by the National Natural Science Foundation of China under Grant 51907155, in part by the Research and Development Plan Projects in Key Area of Guangdong Province under Grant 2020B010170001, in part by the Research and Development Plan Projects in Key Area of Shaanxi Province under Grant 2021GXLH-Z-006, and in part by Civil Aerospace Technology Research Project in Advance under Grant B0202. *(Corresponding author: Xu Yang.)*

The authors are with the State Key Laboratory of Electrical Insulation and Power Equipment, School of Electrical Engineering,, Xi'an Jiaotong University, Xi'an 710049, China (e-mail: wangkp@xjtu.edu.cn; wf626312198@stu.xjtu.edu.cn; wjw020216@stu.xjtu.edu.cn; wujiarui123@stu.xjtu.edu.cn; llwang@xjtu.edu.cn; yangxu@mail.xjtu.edu.cn).

Color versions of one or more figures in this article are available at https://doi.org/10.1109/TPEL.2021.3119770.

Digital Object Identifier 10.1109/TPEL.2021.3119770

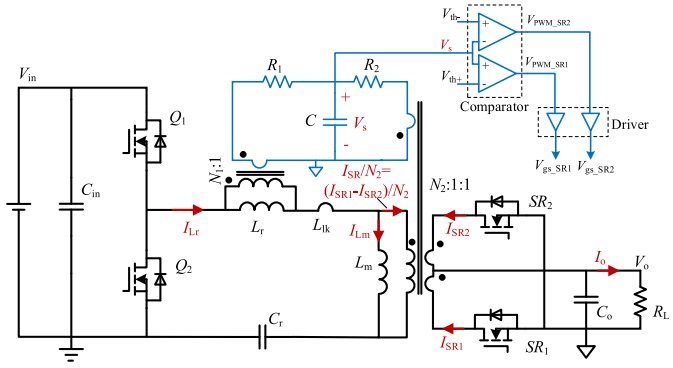


Fig. 1. Proposed SR current detection and SR control method in *LLC* circuit.

is susceptible to noise interference. Another disadvantage of this method is that the ON-resistance varies with temperature, which leads to inaccurate SR current detection. Another popular method is to detect the conduction state of the body diode first and then adaptively adjust the SR control signal accordingly [8], [9]. This method is not a cycle-by-cycle control. Complex transient processes, such as sudden load change, soft start, and short circuit, need to carefully adjust and check the SR control signal. This is time consuming and also increases the control complexity. In addition, more work is required to ensure that the conduction state of the body diode is accurately detected. Commercial SR chips are mainly based on the above two methods, optimized for specific applications. The chips are difficult to extend to applications with Megahertz frequencies or hundreds of amperes. Based on the above analysis, it is still necessary to propose an SR current detection method for synchronous rectification in *LLC* circuits with high frequency, large current, or complex working modes.

This letter presents a method to detect the SR current for cycle-by-cycle SR control. The resonant current and the magnetizing current are detected through magnetic coupling, and then the SR current is obtained by subtracting the two. This method requires only a few passive components and has advantages, such as high bandwidth, strong anti-interference ability, and easy implementation. The working principle is illustrated in detail, and then the proposed method is verified through experiments. The proposed method is applied to SR control in the *LLC* circuit, and it works well. The proposed method is suitable for high frequency and large current situations.

## II. Proposed Method for SR Current Detection

Fig. 1 shows an *LLC* circuit with the proposed SR current detection method. The SR current $I_{\rm SR}$ is proportional to the difference between the resonant current $I_{Lr}$ and the magnetizing current $I_{Lm}$. $I_{Lr}$ and $I_{Lm}$ are measured by magnetic coupling first, and then $I_{\rm SR}$ is obtained by subtracting the two and dividing them by $N_2$. In full-bridge rectification, $I_{\rm SR}$ is the secondary winding current of the transformer; in full-wave rectification, $I_{\rm SR} = I_{\rm SR1} - I_{\rm SR2}$. The SR control signals are obtained by comparing the SR current waveform with threshold voltages. The SR1 control signal $V_{\rm PWM\_SR1}$ is obtained by comparing

TABLE I
Key Parameters

| Parameters | Value | Parameters | Value |
|---|---|---|---|
| $L_r$ | 1.2 μH | $C_r$ | 153 nH |
| $L_m$ | 8.2 μH | $R_1$ | 7.2 kΩ |
| $N_1$ | 3 | $R_2$ | 29.5 kΩ |
| $N_2$ | 5 | $C$ | 1 nF |

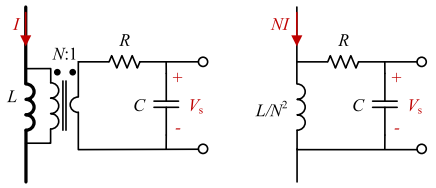


Fig. 2. (a) Circuit of the proposed current detection method. (b) Simplified equivalent circuit.

$V_s$ with a positive threshold voltage $V_{\rm th+}$. Similarly, the SR2 control signal $V_{\rm PWM\_SR2}$ is obtained by comparing $V_s$ with a negative threshold voltage $V_{\rm th-}$. The key parameters used in the following calculations and experiments are given in Table I.

### A. Basic Working Principle

A single-turn detection coil is wound on the magnetic core of the inductor to form an $N$:1 transformer. $N$ is the winding turns of the inductor. A resistor and a capacitor are connected in series to the detection coil. Within a specific frequency range, the voltage on the capacitor is proportional to the inductor current, and there is no phase difference between the two. The circuit is shown in Fig. 2.

According to Fig. 2, the sensed voltage $V_s$ can be derived as

$$V_s = NI \cdot \left[\frac{Ls}{N^2} \parallel \left(R + \frac{1}{Cs}\right)\right] \cdot \frac{\frac{1}{Cs}}{R + \frac{1}{Cs}} = I \cdot \frac{\frac{L}{NRC}}{\frac{Ls}{N^2R} + 1 + \frac{1}{RCs}}. \quad (1)$$

When $Ls/(N^2R) << 1$ and $1/(RCs) << 1$, the gain $G = V_s/I$ can be derived from the above equation as

$$G = \frac{V_s}{I} = \frac{L}{NRC}. \quad (2)$$

The upper corner frequency $\omega_H$ and the lower corner frequency $\omega_L$ can be solved from $Ls/(N^2R) = 1$ and $1/(RCs) = 1$

$$\omega_H = \frac{N^2R}{L} \quad (3)$$

$$\omega_L = \frac{1}{RC}. \quad (4)$$

It can be seen from the above formula that the gain and frequency range can be easily set by $R$ and $C$. The resistance $R$ should take a relatively large value to limit the current flowing through the detection coil, thereby reducing the loss of the detection circuit.

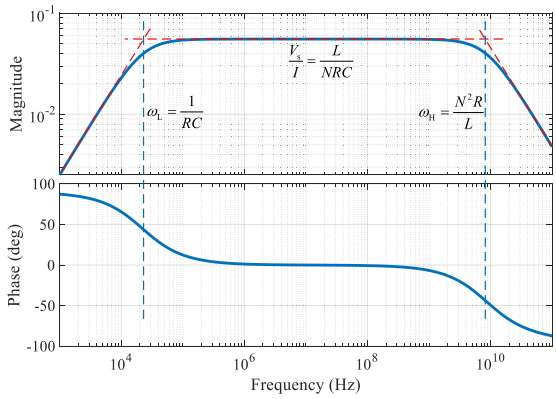


Fig. 3. Gain curve $G = V_s/I$.

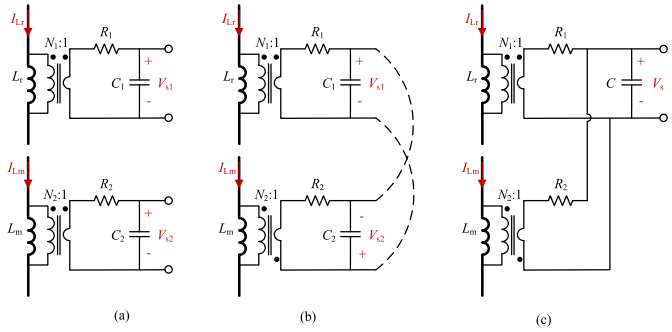


Fig. 4. Proposed SR current detection method.

Fig. 3 gives an example. It can be calculated that $G = 0.056$, $f_H = 8.6$ GHz, and $f_L = 22$ kHz. It can be seen that this method has a very wide frequency range and is suitable for high-frequency applications. The inductance $L$ is the resonant inductance $L_r$ for resonant inductor and is the magnetizing inductance $L_m$ for the transformer.

The resonant current $I_{Lr}$ and the magnetizing current $I_{Lm}$ can be detected separately using the above method. The SR current $I_{\mathrm{SR}}$ is $N_2$ times the difference between the two

$$I_{\mathrm{SR}} = N_2 \left(I_{Lr} - I_{Lm}\right). \tag{5}$$

The subtraction can be implemented with an op-amp. Here, we will introduce a simple method that does not require an op-amp. The polarity of the capacitor voltage can be changed by swapping the terminals of the detection coil. The subtraction is achieved by connecting the circuit in a way, as shown in Fig. 4. Furthermore, the two shared capacitors can be reduced to one. Fig. 5 shows the equivalent circuit. The combined circuit is equivalent to adding a resistor and inductance series load to the original detection circuit. Because the value of the resistor is relatively large, it has little effect on the gain curve in the frequency range of interest.

According to the circuit superposition theorem, the sensed voltage $V_s$ is the addition of the excitation results of the two currents

$$V_s = V_{s1} - V_{s2} = \frac{L_r}{N_1 R_1 C} I_{Lr} - \frac{L_m}{N_2 R_2 C} I_{Lm}. \tag{6}$$

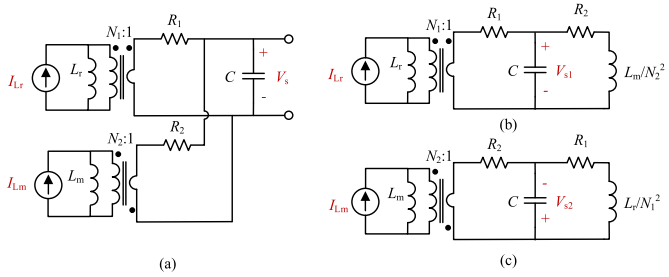


Fig. 5. Equivalent circuit of the proposed SR current detection method.

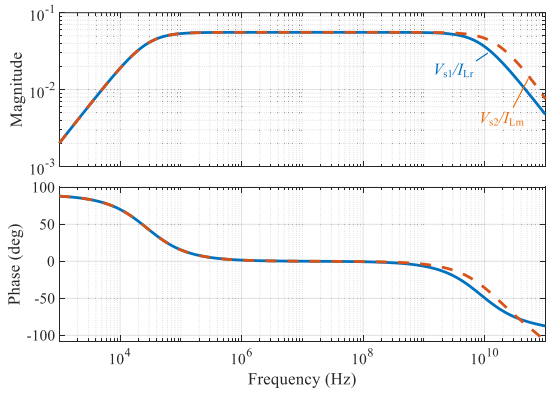


Fig. 6. Gain curves of $G_1 = V_{s1}/I_{Lr}$ and $G_2 = V_{s2}/I_{Lm}$.

By adjusting the values of $R_1$ and $R_2$, we can ensure that the coefficients of $I_{Lr}$ and $I_{Lm}$ in the above formula are equal, that is

$$\frac{R_1}{R_2} = \frac{N_2 L_r}{N_1 L_m}. \tag{7}$$

When $R_1$ and $R_2$ are matched, $V_s$ is proportional to $I_{\mathrm{SR}}$

$$V_s = \frac{L_r}{N_1 R_1 C}\left(I_{Lr} - I_{Lm}\right) = \frac{L_r}{N_1 N_2 R_1 C} I_{\mathrm{SR}}. \tag{8}$$

Fig. 6 shows the gain curves of $G_1 = V_{s1}/I_{Lr}$ and $G_2 = V_{s2}/I_{Lm}$. In the flat region of the gain curves, the two gains are the same: $G_1 = G_2 = 0.056$.

Due to the driving delay in the circuit, the SR channel conduction will lag behind the SR control signal. The driving delay can be compensated to a certain extent by adjusting $R_2$. The delay compensation is analyzed in the time domain as follows. Fig. 7 shows the key waveforms when $f_s \leq f_r$ and $f_s > f_r$. $f_s$ is the switching frequency, and $f_r$ is the resonant frequency ($f_r = 1/\sqrt{L_r C_r}$). Then, we can calculate the sensed voltage $v_s$ in the time domain as

$$v_s(t) = v_{s1}(t) - v_{s2}(t) = \frac{L_r}{N_1 R_1 C} i_{Lr}(t) - \frac{L_m}{N_2 R_2 C} i_{Lm}(t). \tag{9}$$

If $R_2$ is reduced to $R_2'$, $v_{s1}$ will remain unchanged, and $v_{s2}$ will become larger to $v_{s2}'$. As a result, the phase of $v_s'$ is a little ahead of $v_s$, as shown in Fig. 7. The SR control signal is advanced for a short time when $R_2$ is reduced, which can be used to compensate for the driving delay. The scale factor $k = v_{s2}/v_{s2}' = R_2'/R_2$, which is not greater than 1.

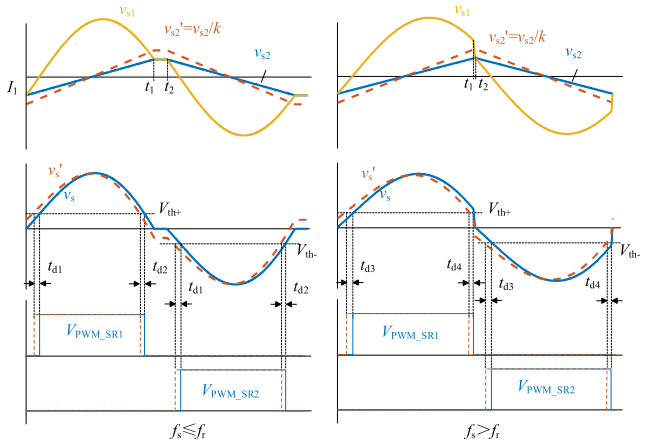


Fig. 7. Waveform adjustment for the driving delay compensation.

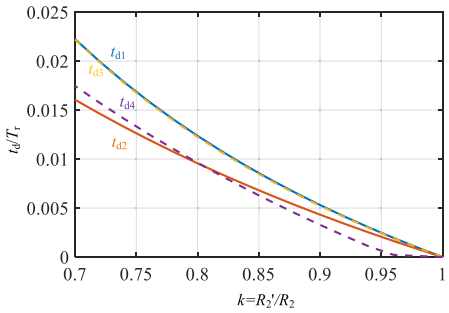


Fig. 8. Curve of delay compensation time as a function of $k = R_2'/R_2$.

The influence of $R_2$ change on the compensation delay time is given in Fig. 8, where $t_d$ is the delay compensation time, and $T_r$ is the resonant period ($T_r = 1/f_r$). It can be seen that the delay compensation time increases as $R_2$ decreases. Therefore, the SR driving delay can be compensated by a proper adjustment of $R_2$.

The sensitivity of the SR current to the resistance tolerance is analyzed as follows. According to (8), the gain $G$ is derived as

$$G = \frac{V_s}{I_{\mathrm{SR}}} = \frac{L_r}{N_1 N_2 R_1 C}. \tag{10}$$

Then, we can obtain the sensitivity of $G$ to $R_1$ as

$$S(G, R_1) = \frac{dG}{dR_1} \cdot \frac{R_1}{G} = -\frac{L_r}{N_1 N_2 R_1^2 C} \cdot \frac{R_1}{G} = -1. \tag{11}$$

If $R_1$ goes up by 1%, then $G$ goes down by 1%. Similarly, the sensitivity of $G$ to other parameters can be derived. The sensitivity of $G$ to $R_2$ is also $-1$.

Here shows a way to match $R_1$ and $R_2$ and get the accurate gain $G$. When the switching frequency is less than the resonant frequency, $I_{\mathrm{SR}}$ should be zero during $t_1$ to $t_2$, as shown in Fig. 7. Using this feature, we can quickly determine whether $R_1$ and $R_2$ are matched in the experiment. If $I_{\mathrm{SR}}$ is not 0 during $t_1$ to $t_2$, $R_1$ and $R_2$ do not match. We can fix $R_1$ first and then adjust $R_2$ until $I_{\mathrm{SR}}$ equals zero during $t_1$ to $t_2$. In the oscilloscope, the average of absolute of $V_s$, that is, avg($|V_s|$), can be easily calculated, and the output current can be measured simultaneously. The ratio of the two avg($|V_s|$)/$I_o$ is the gain $G$. In this way, we can match $R_1$ and $R_2$ and get the gain $G$ accurately without considering the tolerance of circuit parameters.

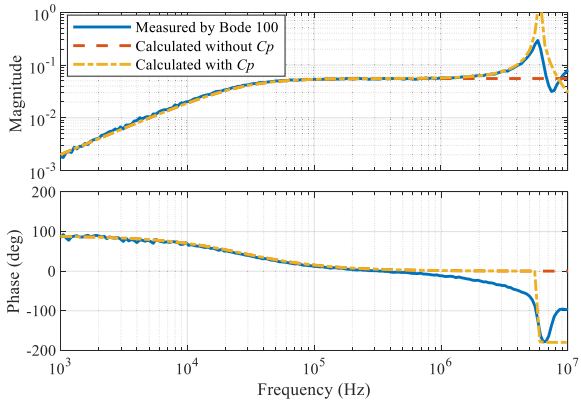


Fig. 9. Measured gain curve $G_1 = V_{s1}/I_{Lr}$.

In addition, if the detection coil is very close to the magnetic winding, the detection signal may be interfered by high *dv*/*dt*. An effective method is to insert a shielding layer between the detection coil and the magnetic winding and then connect the shielding layer to a stable potential point. The shielding layer can bypass the noise to prevent the detection signal from being interfered.

## III. Experimental Verifications

An *LLC* prototype is built to verify the proposed current detection method. The circuit parameters are given in Table I. The output voltage is 10 V, and the rated output current is 50 A. The detection coils are only one turn.

The gain curve is measured using an instrument Bode 100. There are only inductors, transformers, and current detection circuits in the gain curve test, and other components are removed to avoid interference. The measured gain curve $G_1 = V_{s1}/I_{Lr}$ is shown in Fig. 9. The calculated results are also drawn in the figure. It can be seen that the measured result is consistent with the calculation result below 2 MHz. The measured gain curve has a spike at high frequencies caused by the parasitic capacitance of the inductor windings. The spike is successfully predicted by calculation in which a parasitic capacitance $C_p$ is connected in parallel with the inductor. Generally, the switching frequency for *LLC* circuits is much lower than the frequency where the parasitic capacitance works.

The resonant current $I_{Lr}$ is measured as a reference for comparison using the capacitor shunt methods [10]. Three working conditions are measured, where the switching frequency is less than, equal to, and greater than the resonant frequency. As for the magnetizing current and SR current are not easy to measure directly, so they are not displayed here. The reference current and the sensed current by the proposed method are plotted in Fig. 10. The two currents show good agreement under different working conditions.

The resonant current, magnetizing current, and SR current are measured using the proposed method under various working conditions, as shown in Fig. 11. The SR current $I_{\mathrm{SR}}$ is the

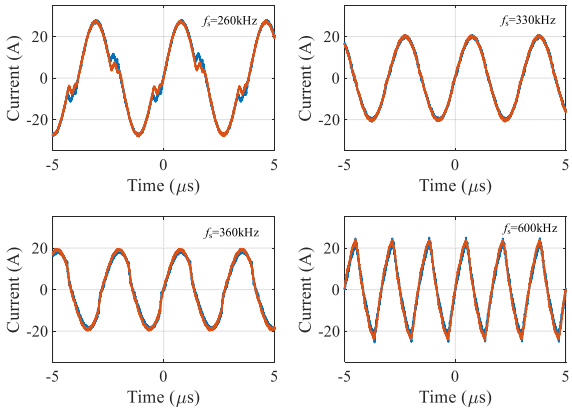


Fig. 10. Waveform comparison of the resonant current under different working conditions. The blue lines are the reference current, and the orange lines are the current waveforms measured by the proposed method.

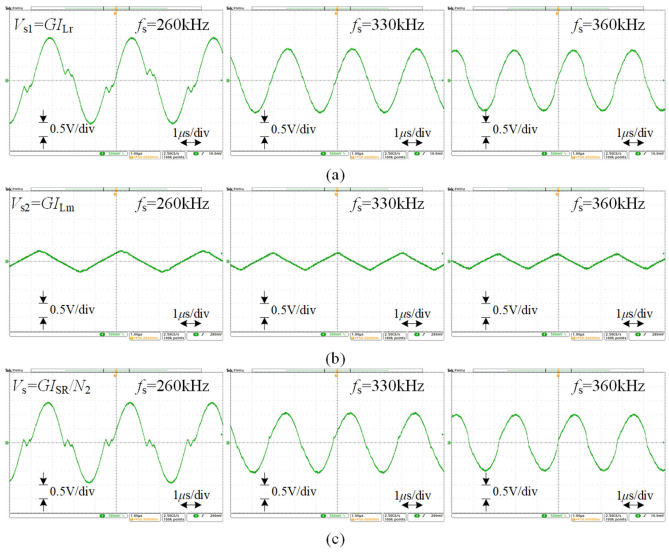


Fig. 11. Current measured by the proposed method. (a) Resonant current. (b) Magnetizing current. (c) SR current.

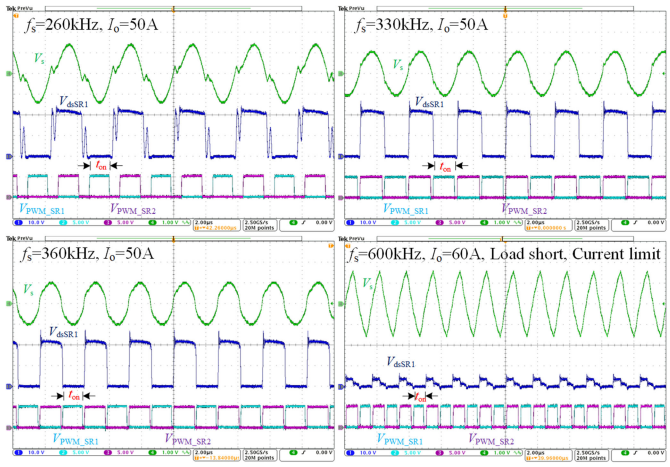


Fig. 12. SR control using the proposed current detection method.

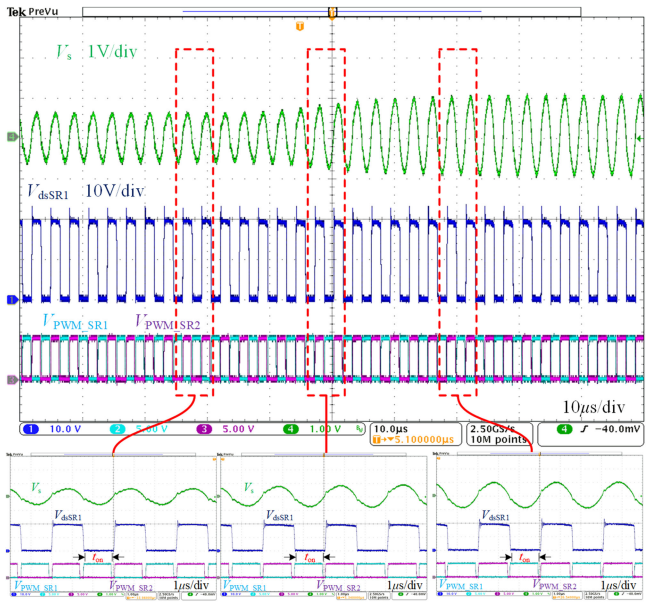


Fig. 13. Proposed SR control during load step-up process.

difference between the inductor current $I_{Lr}$ and the magnetizing current $I_{Lm}$. These waveforms are consistent with the theoretically expected shapes. For example, the magnetizing current has a triangular shape. The SR current is discontinuous when $f_s<f_r$ and is continuous when $f_s\geq f_r$.

The SR control signal is obtained by comparing the detection signal $V_s$ with a threshold voltage. Fig. 12 shows that the SR control works well at different switching frequencies. The switching frequency increases to limit the output current in an overload situation, and the SR control still works well. The waveform $V_s$ is adjusted by reducing $R_2$ properly to compensate for the driving delay. The conduction time of the SRs body diode can be read from the $V_{\mathrm{ds\_SR1}}$ waveforms, as shown in Fig. 12, at different switching frequencies. And then, the ratio of the diode conduction loss $P_{\mathrm{dc}}$ to the SR loss $P_{\mathrm{SR}}$ can be calculated. When the switching frequency is 260 kHz, the loss ratio $P_{\mathrm{dc}}/P_{\mathrm{SR}}$ is only 7.5%. The diode conduction time is further reduced at other switching frequencies, and the loss ratio $P_{\mathrm{dc}}/P_{\mathrm{SR}}$ is less than 3%.

Fig. 13 shows the proposed SR control during the load step-up process. The SR control works well both in the steady-state and transient processes. Fig. 14 shows the proposed SR control during the overload current limiting process. The switching frequency increases to 600 kHz, and the load current is limited to about 60 A. The SR control works well throughout the process.

The average absolute of $I_{\mathrm{SR}}$ is equal to the output current $I_o$, $\mathrm{avg}(|I_{\mathrm{SR}}|)=I_o$. Therefore, we can get $I_o$ from $V_s$ after rectifying and filtering, namely $\mathrm{avg}(|V_s|)$. It can be derived that $\mathrm{avg}(|V_s|)/I_o=\mathrm{avg}(|GI_{\mathrm{SR}}/N_2|)/I_o=G/N_2$. Fig. 15 shows the curve of $k\cdot\mathrm{avg}(|V_s|)$ varying with $I_o$, which has excellent linearity. Therefore, the output current signal can be obtained from $V_s$. In this way, we can save an additional output current detection circuit, which usually has a large loss and size in high-current applications. Moreover, the slope of $k\cdot\mathrm{avg}(|V_s|)/I_o$

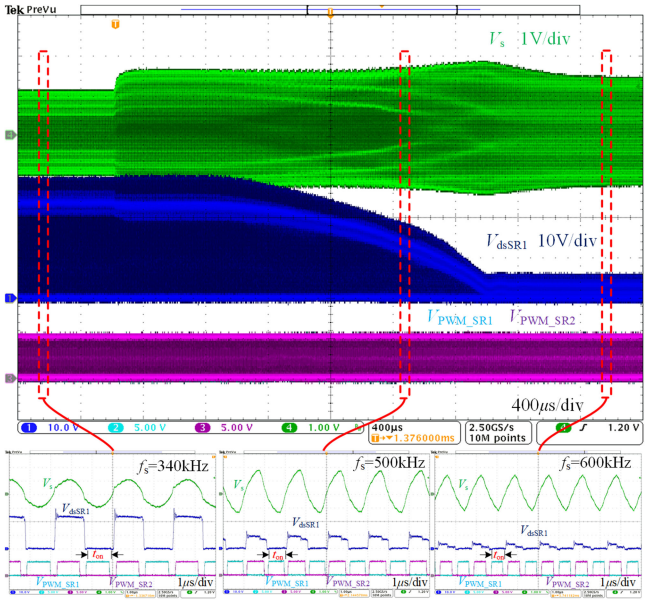


Fig. 14. Proposed SR control during overload current limiting process.

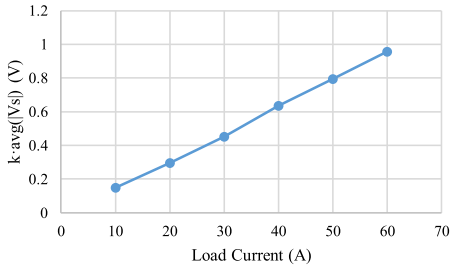


Fig. 15. Measured avg($|V_s|$) is proportional to the output current $I_o$.

is 0.016, which is close to the calculated result $k{\cdot}G/N_2 = 1.5{\times}0.056/5 = 0.017$. The coefficient $k$ is the magnification of $V_s$ during rectification and filtering, and its value is equal to 1.5. This further proves that the measurement results are accurate.

## IV. Conclusion

This letter proposed a method to detect the SR current for cycle-by-cycle SR control. The proposed method can detect the resonant current and the magnetizing current with few passive components and then obtain the SR current. The proposed method has advantages, such as high bandwidth, strong anti-interference ability, and easy implementation. Finally, the proposed method is verified through experiments, and it works well for *LLC* SR control at high frequency and large current situations. In addition, the output current signal can be obtained through the proposed method.

## References

[1] F. C. Lee, Q. Li, and A. Nabih, "High frequency resonant converters: An overview on the magnetic design and control methods," *IEEE J. Emerg. Sel. Topics Power Electron.*, vol. 9, no. 1, pp. 11–23, Feb. 2021.

[2] M. H. Ahmed, A. Nabih, F. C. Lee, and Q. Li, "Low-loss integrated inductor and transformer structure and application in regulated LLC converter for 48-V bus converter," *IEEE J. Emerg. Sel. Topics Power Electron.*, vol. 8, no. 1, pp. 589–600, Mar. 2020.

[3] W. Zhang, F. Wang, D. J. Costinett, L. M. Tolbert, and B. J. Blalock, "Investigation of gallium nitride devices in high-frequency LLC resonant converters," *IEEE Trans. Power Electron.*, vol. 32, no. 1, pp. 571–583, Jan. 2017.

[4] Y. Wei, Q. Luo, and H. A. Mantooth, "Synchronous rectification for LLC resonant converter: An overview," *IEEE Trans. Power Electron.*, vol. 36, no. 6, pp. 7264–7280, Jun. 2021.

[5] K. Wang, H. Li, Z. Yu, L. Wang, X. Yang, and A. Qiu, "An isolated capacitor-compensated current sensing method for high-frequency resonant converters," *IEEE Trans. Power Electron.*, vol. 34, no. 7, pp. 6009–6013, Jul. 2019.

[6] D. Wang and Y.-F. Liu, "A zero-crossing noise filter for driving synchronous rectifiers of LLC resonant converter," *IEEE Trans. Power Electron.*, vol. 29, no. 4, pp. 1953–1965, Apr. 2014.

[7] L. He, J. Chen, B. Cheng, and H. Zhou, "Duty cycle loss compensation method based on magnetic flux cancelation in high-current high-frequency synchronous rectifier of LCLC converter," *IEEE Trans. Power Electron.*, vol. 36, no. 1, pp. 103–113, Jan. 2021.

[8] W. Feng, F. C. Lee, P. Mattavelli, and D. Huang, "A universal adaptive driving scheme for synchronous rectification in LLC resonant converters," *IEEE Trans. Power Electron.*, vol. 27, no. 8, pp. 3775–3781, Aug. 2012.

[9] C. Fei, Q. Li, and F. C. Lee, "Digital implementation of adaptive synchronous rectifier (SR) driving scheme for high-frequency LLC converters with microcontroller," *IEEE Trans. Power Electron.*, vol. 33, no. 6, pp. 5351–5361, Jun. 2018.

[10] STMicroelectronics, "Enhanced high voltage resonant controller L6699," Geneva, Switzerland, 2013. [Online]. Available: www.st.com